Ultrathin single crystal Pt nanowires grown on N-doped carbon nanotubes†

Shuhui Sun,[a] Gaixia Zhang,[a] Yu Zhong,[a] Hao Liu,[a] Ruying Li,[a] Xiaorong Zhou[b] and Xueliang Sun*[a]

Received (in Cambridge, UK) 5th August 2009, Accepted 22nd September 2009
First published as an Advance Article on the web 13th October 2009
DOI: 10.1039/b916080a

Ultrathin single crystal platinum nanowires with diameters of ~2.5 nm and lengths up to 100 nm were synthesized on nitrogen-doped CNTs (N-CNTs) *via* a straightforward wet-chemical method in environmentally friendly water solution at room temperature, without using any stabilizing agent. These ultrathin nanowires and their composites with N-CNTs hold potential for a wide range of applications.

Among various one-dimensional (1D) noble metal nanostructures, platinum nanowires (Pt NWs) are of particular importance and are expected to play a critical role in electronics, catalysis, fuel cells and the automotive industries, as this metal has outstanding catalytic and electrical properties and superior resistance to corrosion.[1,2] To date, various methods have been developed for the synthesis of Pt NWs. However, wet-chemical methods often lead to the formation of relatively large diameter (>10 nm) or polycrystalline wires whereas the commonly used template approach has problems associated with the removal of the template.[3] It is well accepted that the surface area increases with the diameter decrease of individual wire, which in turn, has immediate effect on surface-related applications.[4] There is very limited success in producing ultrafine Pt NWs, especially on the scale below 5 nm.[5] Very recently, a flurry of papers has appeared in the literature regarding the synthesis of Au ultrathin (<3 nm) NWs.[6] However, the synthesis of ultrathin NWs of single crystal Pt with such small diameters is still challenging.

Recently, nitrogen-doped carbon nanotubes (N-CNTs) have attracted much attention due to their unique properties and wide applications.[7] Specifically, they have been widely used as diverse matrices to fabricate various nanocomposites such as Pt/N-CNTs, which possess great potential in fuel cells, electronic devices, and chemical sensors.[8]

Here we report a straightforward solution method for the synthesis of single crystalline ultrathin Pt NWs, with uniform diameters of ~2.5 nm and lengths up to 100 nm, on N-CNTs. In addition, direct evidence for the formation of ultrathin Pt NWs was provided by systematically investigating their growth process, and the key role of nitrogen was revealed. The synthetic procedure is very simple, and only two chemicals (H_2PtCl_6 and HCOOH) were used throughout the whole synthetic process, without using any stabilizing agent. Further, the reaction was conducted at room temperature in environmentally friendly aqueous solution.

In a typical synthesis, 0.032 g hexachloroplatinic acid ($H_2PtCl_6{\cdot}6H_2O$, Aldrich) and 1 mL formic acid (HCOOH, Aldrich) were added simultaneously to 20 mL H_2O to form a golden orange solution. The N-CNTs (nitrogen content of 10.4 at.%) grown on carbon paper, synthesized by a CVD method,[9] were immersed in the above solution, acting as the growth substrates. Then the reaction proceeded at room temperature without stirring for up to 3 days until the solution color gradually changed to colorless. The final product can be easily collected by handling the carbon paper support and washing with deionized water.

Fig. 1 shows the representative transmission electron microscopy (TEM) images of N-CNTs before and after growth of the Pt NWs. It can be seen that the pristine N-CNTs have diameters ranging from 40 to 60 nm (Fig. 1A, and Fig. S1, ESI†), and the bamboo-like structure can be attributed to the integration of N into the graphitic structure.[7] Fig. 1B shows that numerous Pt NWs, with lengths up to 100 nm, grow uniformly on N-CNTs, forming a hybrid structure of Pt NWs/N-CNTs. The higher magnification image (Fig. 1C) indicates that the diameter of the Pt NWs is less than 3 nm. The aspect ratio of Pt NWs easily approaches 50. A survey of several tens of Pt NWs under TEM investigation reveals that the diameters of these NWs are in the range of 2 to 3 nm, with an average of 2.5 nm. Besides the ultrathin nature, these Pt NWs are also single crystalline. Selected area electron diffraction (SAED) pattern recorded from a few NWs confirms their high crystallinity (inset in Fig. 1C). The high-resolution TEM (HRTEM) image (Fig. 1D) shows that the Pt NWs grow along ⟨111⟩ direction, and the interplanar distance between the {111} planes is 0.23 nm which matches that for bulk Pt crystals. To the best of our knowledge, this is the first time that single crystal Pt NWs with such thin diameters were synthesized with such a simple method. Interestingly, our previous work shows that under similar synthetic conditions but without using N-incorporated supports, Pt NWs that grew either freely in solution or on CNT and carbon black supports, always have relative larger diameters of 4 nm[2b,5b,c] (also see Fig. S2–S4, ESI†). These reveal that N-doping into CNTs is crucial to the formation of ultrathin Pt NWs with diameter less than 3 nm.

[a] *Department of Mechanical and Materials Engineering, The University of Western Ontario, London, ON, Canada N6A 5B9. E-mail: xsun@eng.uwo.ca; Fax: +1-519-661-2111 ext. 87759; Tel: +1-519-661-3020*
[b] *School of Materials, University of Manchester, Manchester, UK M60 1QD*

† Electronic supplementary information (ESI) available: SEM images of pristine N-CNTs; SEM and TEM images of Pt NWs grew freely and on CNT as well as CB supports; XPS peak separation of Pt4f. See DOI: 10.1039/b916080a

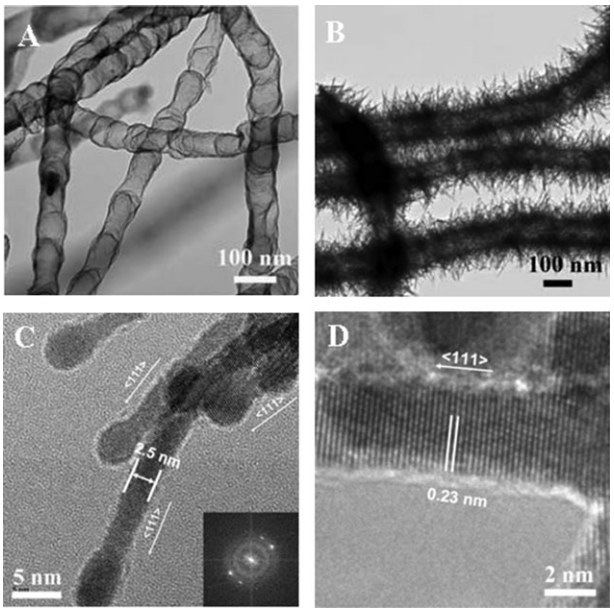

Fig. 1 TEM images of N-CNTs before (A) and after (B) the growth of Pt NWs; TEM (C) and HRTEM (D) images of ultrathin Pt NWs.

In order to investigate the possible reasons for the formation of ultrathin Pt NWs on N-CNTs, X-ray photoelectron spectroscopy (XPS) was employed to study the chemical composition and status of the product. The asymmetric C1s high-resolution spectrum (Fig. 2A, centered at ~285 eV) is deconvoluted into five peaks, which can be assigned, respectively, to the C–C bonds in graphite (PC1), alternate defect carbon structures associated with C–N and C–O bonds overlapping (286–289 eV, PC2–4), and PC1 $\pi^* \leftarrow \pi$ shake-up satellite (PC5). Comparing the carbon spectra before and after Pt growth (inset of Fig. 2A), the latter one shows a narrower band with significant decrease of PC2–4 peaks corresponding to the localized (defect) carbon atoms,[11] which can be attributed to the block effect of Pt NWs to the X-ray. This indicates that Pt NWs are more easy to deposit on the defects of the N-CNTs than on the perfect graphite structures. The deconvolution of the Pt4f spectrum (Fig. S5, ESI†) indicates pure metallic Pt, without obvious carbide and nitride formation. Fig. 2B shows the N1s spectra of the N-CNTs before and after Pt deposition. The pristine N1s spectrum was deconvoluted into 5 peaks.[10] It is believed that the main peak (398.7 eV) corresponding to the pyridine-like N within the predominantly graphitic framework is responsible for both the wall roughness and interlinked morphologies observed in the N-doped structure.[11] After Pt deposition, in addition to the significant decrease of the whole N1s signal and the almost complete disappearance of two peaks corresponding to the oxide N atoms (403–405 eV), the area ratio of pyridine-like (398.7 eV) to graphite-like (401.0 eV) N decreased from 1.81 to 1.21, further implying that Pt NWs grow preferentially on the defect sites that more associated with pyridine N, of the N-CNTs.

The distribution of nitrogen and carbon in the N-CNTs was studied by elemental mapping using electron energy loss spectroscopy (EELS) (Fig. 3). The brighter regions represent a higher concentration of the element. Fig. 3C shows that while the N atoms seem to be present throughout of the

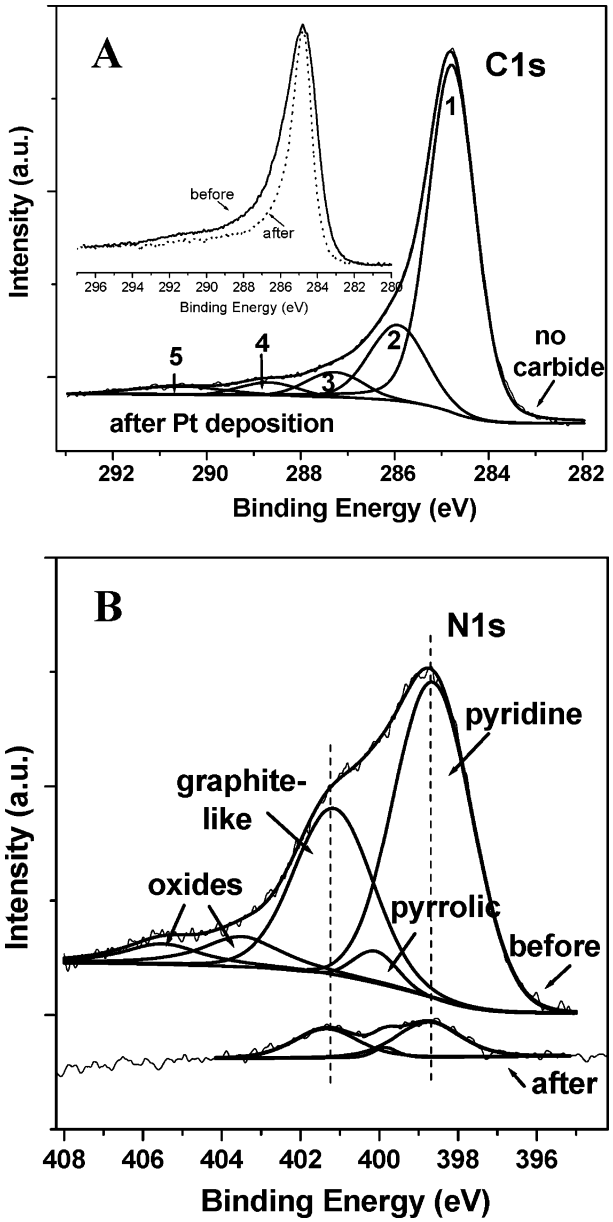

Fig. 2 Typical XPS spectra of N-CNTs before and after Pt deposition. (A) C1s, and (B) N1s.

N-CNTs, they are more prevalent on the wall ruffles and the interlinked parts (nodes) of N-CNTs which may be assigned mainly to the pyridine-like N.[11] This is consistent with our XPS results since much higher concentration pyridine-like than other types N was detected in pristine N-CNTs. According to our XPS results, these defects induced by N incorporation would provide preferred anchoring sites for Pt deposition.

To reveal the underlying growth mechanism of ultrathin Pt NWs on N-CNTs, products were collected as a function of growth time, and their morphologies were evaluated by TEM and HRTEM. The HRTEM image of a pristine N-CNT (Fig. 4A) shows that the intersects are usually consist of 4–6 graphitic layers. Between these intersects, there are many irregular web-like structures (2–3 atomic layers) across the surface. Careful inspection reveals the existence of many broken graphitic layers (defects) along the entire surface of

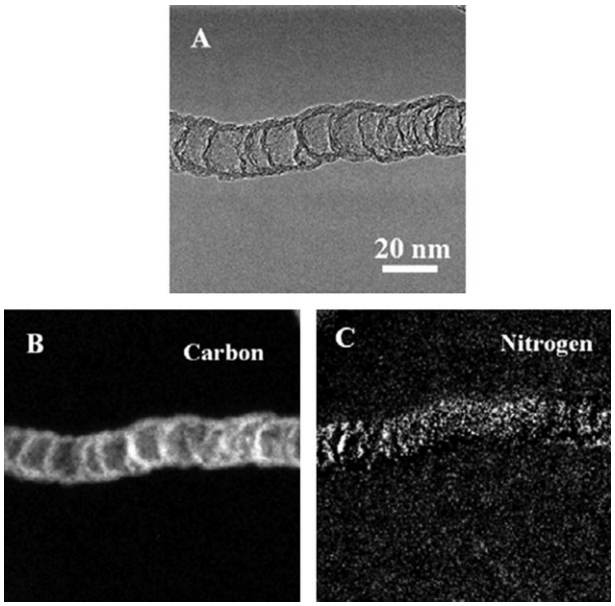

Fig. 3 EELS mapping of a pristine N-doped CNT: (A) bright field image; (B) carbon map; (C) nitrogen map.

the nanotube, suggesting that N incorporation into CNTs promotes not only the bamboo-structured morphology but also strongly affects the tube defect structure. At the initial growth stage (Fig. 4B and inset), Pt nuclei readily attach to the sites with higher density defects along the N-CNTs, since nitrogen can enhance the Pt adsorption on the CNT surface due to its large electron affinity.[12] Interestingly, the size of the Pt nanoparticles (nuclei) ranges from 2 to 3 nm with an average of 2.5 nm, which is smaller than those on carbon nanotubes and nanospheres. We believed that the broken graphitic layers, which are more associated with the pyridinic N, confine the Pt atoms and provide the main initial nucleation sites for the formation of Pt nanoparticles with small diameters. This may be the key for the formation of ultrathin Pt NWs on N-CNTs. As the growth time increased, a large amount of nanoparticles progressively cover the whole surface of the N-CNTs. These small Pt nuclei act as the seeds to direct the anisotropic growth of Pt NWs, in that the growth rate along the closed-packed ⟨111⟩ direction is enhanced at very slow reduction rate,[5] forming Pt NW/N-CNT hybrid novel structures (Fig. 4C and D).

In conclusion, ultrathin (2–3 nm in diameter) Pt NWs have been synthesized on N-CNTs by a very simple aqueous solution method at room temperature. It is believed that the widely distributed defects, associated with N incorporation, on the N-CNTs surface, confine the Pt atoms and play a key role in the formation of the tiny nuclei that further leads to the anisotropic growth of ultrathin nanowires. This simple synthetic strategy and the underlying mechanism could give new insight into the synthesis of other metal nanowires with dimensions similar to those reported here. Isolated ultrathin nanowires could be obtained if the N-CNT supports were deliberately removed. These ultrathin nanowires and their composites with N-CNTs hold potential for catalysis, fuel cells and electrochemical sensors.

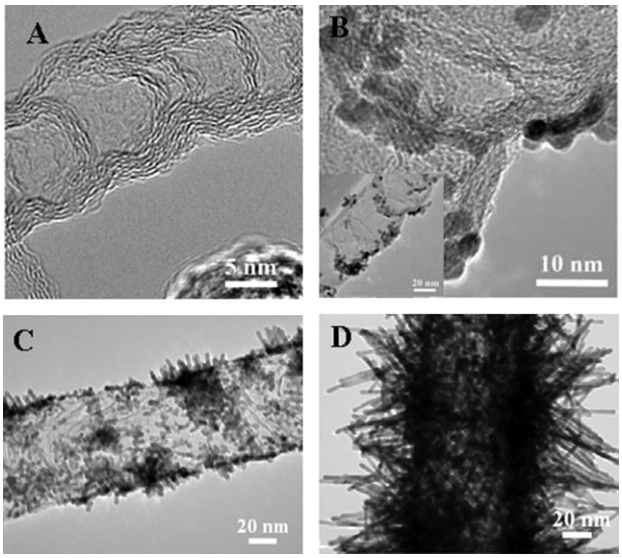

Fig. 4 TEM images show the growth process of ultrathin Pt NWs on N-CNTs. (A) pristine N-CNT; (B) initial (nuclei), (C) intermediate and (D) final growth stages.

This work was supported by NSERC, CRC, CFI, ORF, ERA and UWO. S.S. is grateful to the NSERC scholarship. G.Z. thanks Ontario PDF program. We are in debt to David Tweddell for his kind help and fruitful discussion.

Notes and references

1 H. A. Gasteiger, S. S. Kocha, B. Sompalli and F. T. Wagner, *Appl. Catal., B*, 2005, **56**, 9.
2 (*a*) W. Lu, B. Mi, M. C. W. Chan, Z. Hui, C. Che, N. Zhu and S. T. Lee, *J. Am. Chem. Soc.*, 2004, **126**, 4958; (*b*) S. Sun, F. Jaouen and J. P. Dodelet, *Adv. Mater.*, 2008, **20**, 3900.
3 Y. Xia, P. Yang, Y. Sun, Y. Wu, B. Mayers, B. Gates, Y. Yin, F. Kim and H. Yan, *Adv. Mater.*, 2003, **15**, 353.
4 L. Cademartiri and G. A. Ozin, *Adv. Mater.*, 2009, **21**, 1013.
5 (*a*) J. Chen, T. Herricks, M. Geissler and Y. Xia, *J. Am. Chem. Soc.*, 2004, **126**, 10854; (*b*) S. Sun, D. Yang, D. Villers, G. Zhang, E. Sacher and J. P. Dodelet, *Adv. Mater.*, 2008, **20**, 571; (*c*) S. Sun, D. Yang, G. Zhang, E. Sacher and J. P. Dodelet, *Chem. Mater.*, 2007, **19**, 6376.
6 (*a*) C. Wang, Y. Hu, C. M. Lieber and S. Sun, *J. Am. Chem. Soc.*, 2008, **130**, 8902; (*b*) Z. Huo, C. Tsung, W. Huang, X. Zhang and P. Yang, *Nano Lett.*, 2008, **8**, 2041; (*c*) X. Lu, M. Yavuz, H. Tuan, B. A. Korgel and Y. Xia, *J. Am. Chem. Soc.*, 2008, **130**, 8900; (*d*) N. Pazos-Pérez, D. Baranov, S. Irsen, M. Hilgendorff, L. M. Liz-Marzan and M. Giersig, *Langmuir*, 2008, **24**, 9855; (*e*) Z. Li, J. Tao, X. Lu, Y. Zhu and Y. Xia, *Nano Lett.*, 2008, **8**, 3052; (*f*) H. Feng, Y. Yang, Y. You, G. Li, J. Guo, T. Yu, Z. Shen, T. Wu and B. Xing, *Chem. Commun.*, 2009, 1984.
7 K. Gong, F. Du, Z. Xia, M. Durstock and L. Dai, *Science*, 2009, **323**, 760.
8 M. Saha, R. Li, X. Sun and S. Ye, *Electrochem. Commun.*, 2009, **11**, 438.
9 S. Trasobares, O. Stephan, C. Colliex, W. K. Hsu, H. W. Kroto and D. R. M. Walton, *J. Chem. Phys.*, 2002, **116**, 8966.
10 (*a*) S. van Dommele, A. Romero-Izquirdo, R. Brydson, K. P. de Jong and J. H. Bitter, *Carbon*, 2008, **46**, 138; (*b*) H. C. Choi, S. Y. Bae, W. S. Jang, J. Park, H. Song, H. J. Shin, H. Jung and J. P. Ahn, *J. Phys. Chem. B*, 2005, **109**, 1683.
11 J. Liu, S. Webster and D. L. Carroll, *J. Phys. Chem. B*, 2005, **109**, 15769.
12 Y. Li, T. Hung and C. Chen, *Carbon*, 2009, **47**, 850.

